

SLAC/INFN Summer Exchange Program 2016
July 11- September 09

ANNUAL GAMMA-RAYSOURCE VARIABILTY

Federica Guidi
Supervisor: Elena Orlando

Abstract

The analysis carried out in these two months at SLAC has been finalized to identify the annual variability of the sky, based on seven year of Fermi-LAT data (08/2008 – 08/2015). Maps of counts normalized with the exposure have been realized for the all sky, for each year and for the integrated seven years. By viewing subsequently the annual images the variability of the sources is evident. An accurate analysis has been done studying the annual counts maps (not normalized with the exposure), smoothed with the Fermi-LAT PSF, in comparison to the 7-year counts map (normalized at one year of exposure), assumed as the expected value of gamma counts. We found 87 sources with a significant variation ($>5\sigma$), that were collected in a catalog called VAR catalog. The sources in our new-generated catalog have been spatially compared with the 3FGL catalog. All the sources in our catalog have found to have a 3FGL counterpart, except one. Moreover we found that all the sources are of extragalactic origin.

Motivations

All-sky variations have been investigated to study long-term variability, and this was never done before. This analysis is model independent so it is not affected by uncertainties on the model of the diffuse emission. Then, we focused on the inner region of the Galaxy, looking for detection of variability above the confusing diffuse emission.

Fermi-LAT all-sky maps

The analysis described in this report is based on 7-year Fermi-LAT Pass8 data, from August 2008 to August 2015, cleaned by GRBs and solar flares.

Fermi-LAT data need to be cleaned and appropriately selected. Specific cuts and various energy ranges have been tested to find the optimal data selection and pixel resolution. In the following are there the maps with energy range [1-500] GeV, $z_{\max}=90\text{deg}$, event type=FRONT and BACK, event class=128 (source), pixel bin size=0.5 deg.

Counts normalized with the exposure maps have been realized for the all-sky, one for each year of observation.

map 1 → 2008/08-2009/08

map 2 → 2009/08-2010/08

map 3 → 010/08-2011/08

map 4 → 2011/08-2012/08

map 5 → 2012/08-2013/08

map 6 → 2013/08-2014/08

map 7 → 2014/08-2015/08

Tools used: Fermi Science Tools, fv, ds9

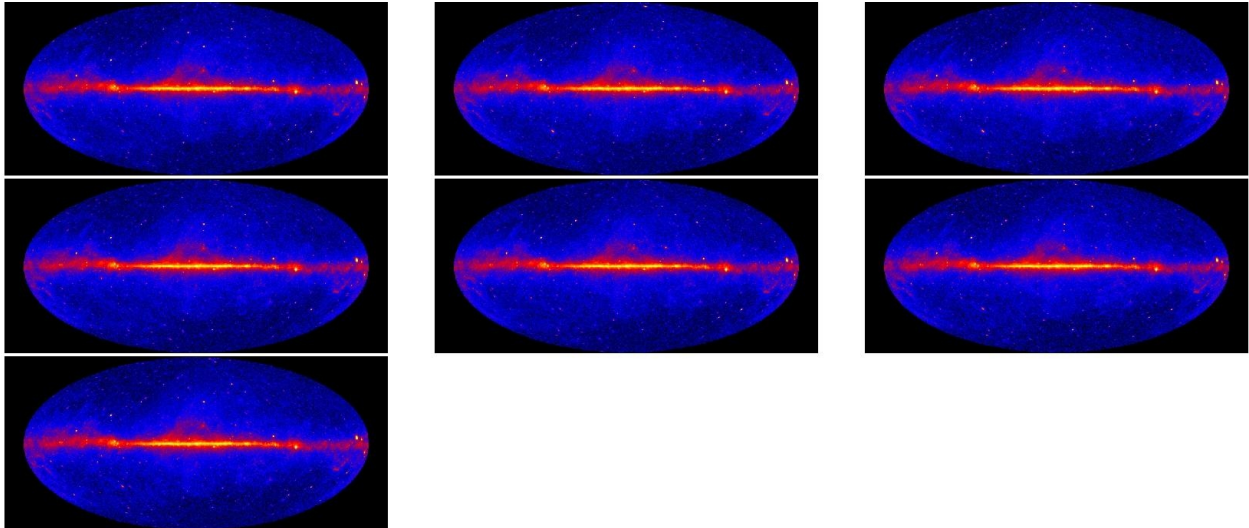


IMAGE 1. Annual maps of counts normalized with the exposure. From left to right map1-map2-map3, map4-map5-map6, map7. Energy range [1-500]GeV, $z_{max}=90deg$, event type=FRONT and BACK, event class=128 (source), 0.5 deg bin size.

Then a map for the entire seven-year data has been produced:

7y map → 2008/08-2015/08

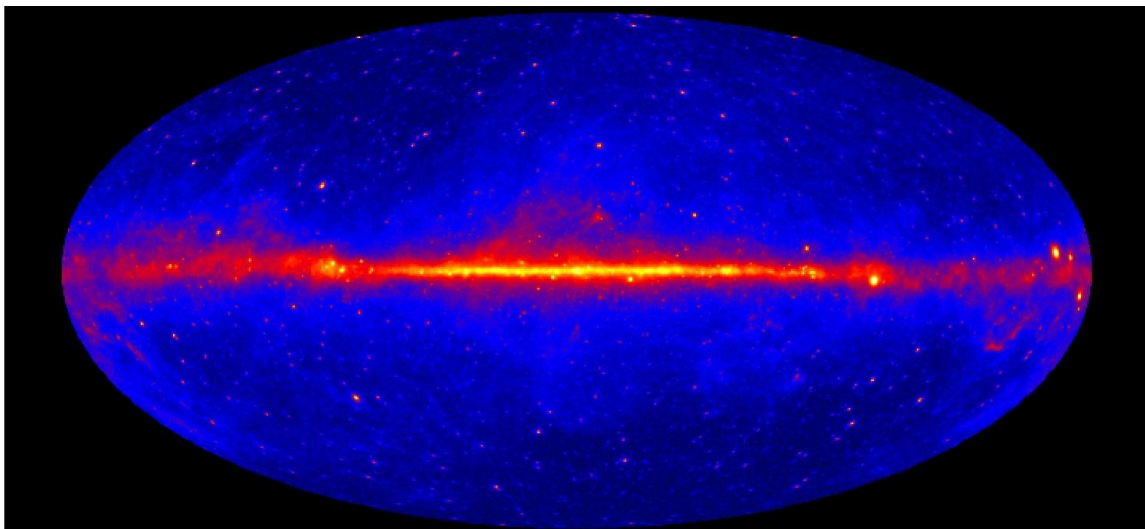


IMAGE 2. 7 year map of counts normalized with the exposure. Energy range [1-500]GeV, $z_{max}=90deg$, event type=FRONT and BACK, event class=128 (source), 0.5 deg bin size.

Fermi-LAT PSF smoothing

The detected direction of provenience of a gamma ray is influenced by the PSF of the instrument, which depends by the energy of the photons observed. A photon detected in the

position (α, δ) of the sky may come, with a certain probability, from a circular region of the sky centered in (α, δ) with radius the characteristic width of the instrument's PSF, that we can call Δ .

The total PSF of the LAT instrument at 1GeV and with a confidence of 68% is $\Delta \approx 0.8 \text{ deg}$.

Since the binning size of the counts maps is smaller than the width of the PSF (0.5 deg), the PSF contribution has been taken into account building a normalized filter mask based on Fermi-LAT PSF function at 1GeV, and convolving the counts map with it.

All the counts maps hereafter are smoothed with the Fermi-LAT PSF.

Tool used: Fermi Science Tools, python, ds9.

Difference and Significance maps

Observing by eye the annual counts maps normalized with exposure maps in sequence it is already possible to identify the variation of some sources. For a more quantitative evaluation of the annual variability of the sky, the 7-year counts map, normalized at one year of exposure as in formula (2), has been assumed as the expected value of gamma counts. The differences between each annual map and the 7-year map have been computed as

$$\text{Diff map} = \text{Count}_{y_i} - \text{Count}_{7_y} \quad (1)$$

where

$$\text{Count}_{7_y} = \text{TotCounts}_{7_y} \frac{\text{exposure}_{y_i}}{\text{exposure}_{7_y}} \quad (2)$$

In the maps of the differences the annual variations have to emerge from the annually static average background.

To consider which variations are significant, the uncertainty associate to the difference has been evaluated. The estimation of the error is based on the statistical fluctuation of the counts map normalized with the exposure:

$$\Delta(\text{Counts}_{y_i} - \text{Counts}_{7_y}) = \sqrt{\text{Counts}_{y_i} + \text{Counts}_{7_y} \left(\frac{\text{exposure}_{y_i}}{\text{exposure}_{7_y}} \right)^2} \quad (3)$$

A more precise estimation of the error has been done by Li & Ma and is summarized in the following formula.

$$S = \frac{\text{Counts}_{y_i} - \text{Counts}_{7_y}}{\Delta(\text{Counts}_{y_i} - \text{Counts}_{7_y})} = \sqrt{2} \left[\text{Counts}_{y_i} \ln \left[\frac{1+a}{a} \frac{\text{Counts}_{y_i}}{\text{Counts}_{y_i} + \text{Counts}_{7_y}} \right] + \text{Counts}_{7_y} \ln \left[\frac{(1+a) \text{Counts}_{7_y}}{\text{Counts}_{y_i} + \text{Counts}_{7_y}} \right] \right] \quad (4)$$

where

$$a = \frac{\text{exposure}_{y_i}}{\text{exposure}_{y_7}}$$

A value of the significance over 5 corresponds to sources with a significant annual variation.

Tool used: Fermi Science Tools, python, fv, ds9.

The difference maps, the error maps and the significant maps for each year are in the images 3-5.

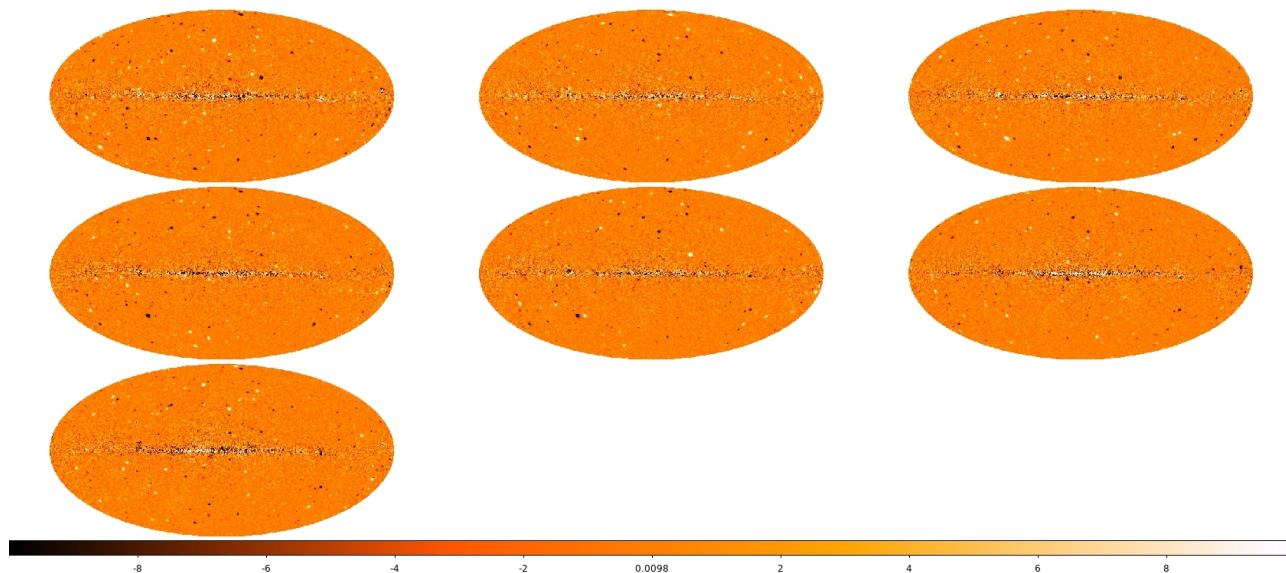


IMAGE 3. Annual maps of counts difference by (1) and (2). From left to right map1-map2-map3, map4-map5-map6, map7.

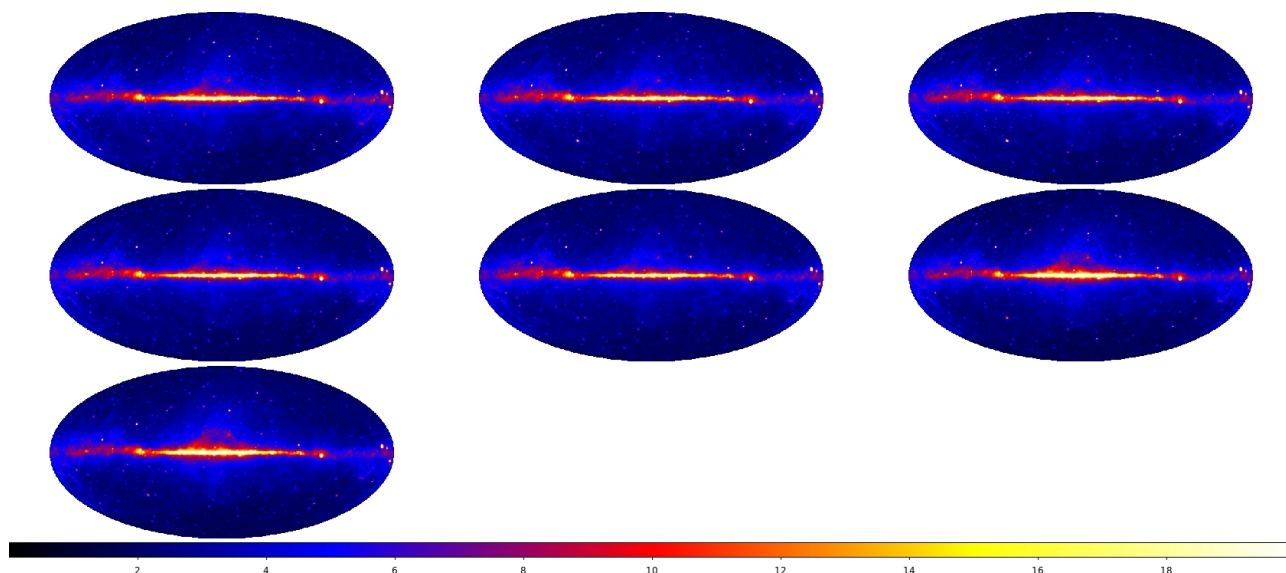


IMAGE 4. Annual maps of counts difference uncertainty from (3). From left to right map1-map2-map3, map4-map5-map6, map7.

On the difference map we can see the sources which have had an annual variation. In correspondence to the Galactic plane there is a fluctuation. Taking into account the error, we can see which sources vary significantly. Furthermore, the fluctuation of the galactic plane is only statistical because the error is big on the galactic plane. This consideration are evident in the significance maps.

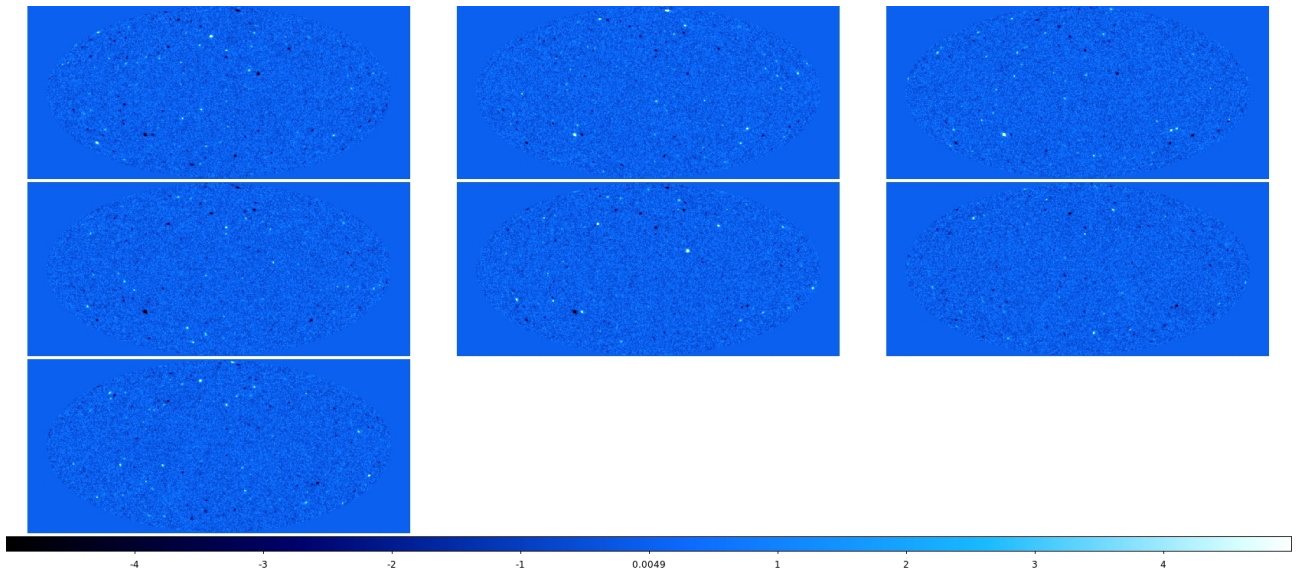


IMAGE 5. Annual significance maps. From left to right map1-map2-map3, map4-map5-map6, map7.

The following image represents the pixel distribution in the first year significance map. The regular distribution around zero of the pixel values is evident. The tale of the distribution over 5 corresponds to the sources of interest.

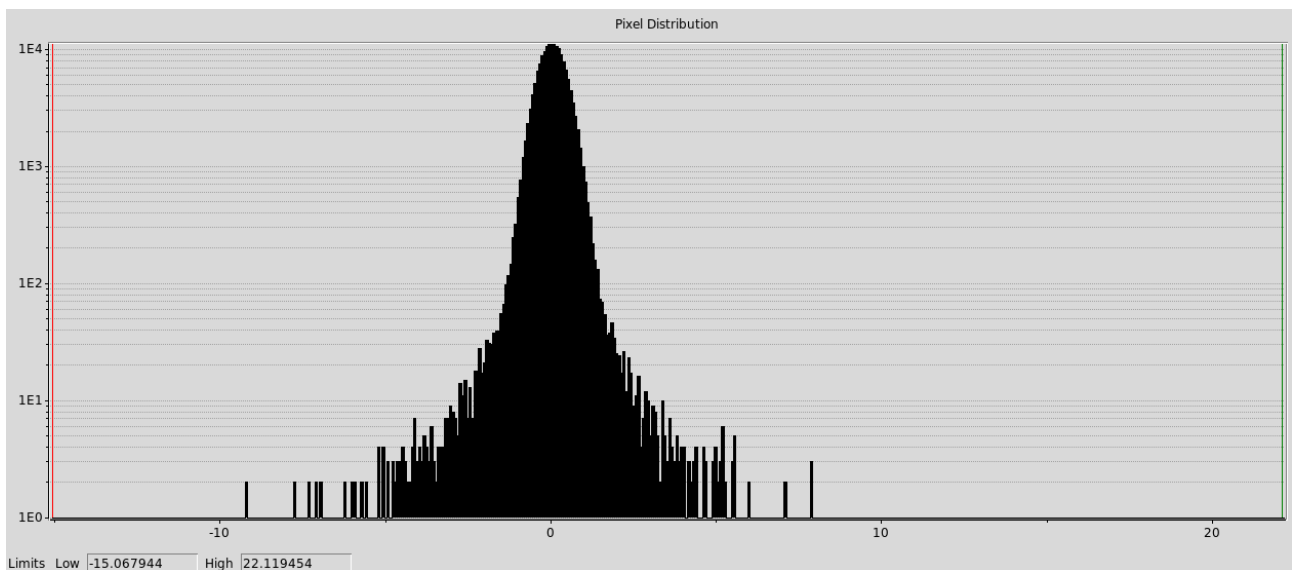


IMAGE 6. Pixel distribution of the first significance map.

Extraction of the variable sources

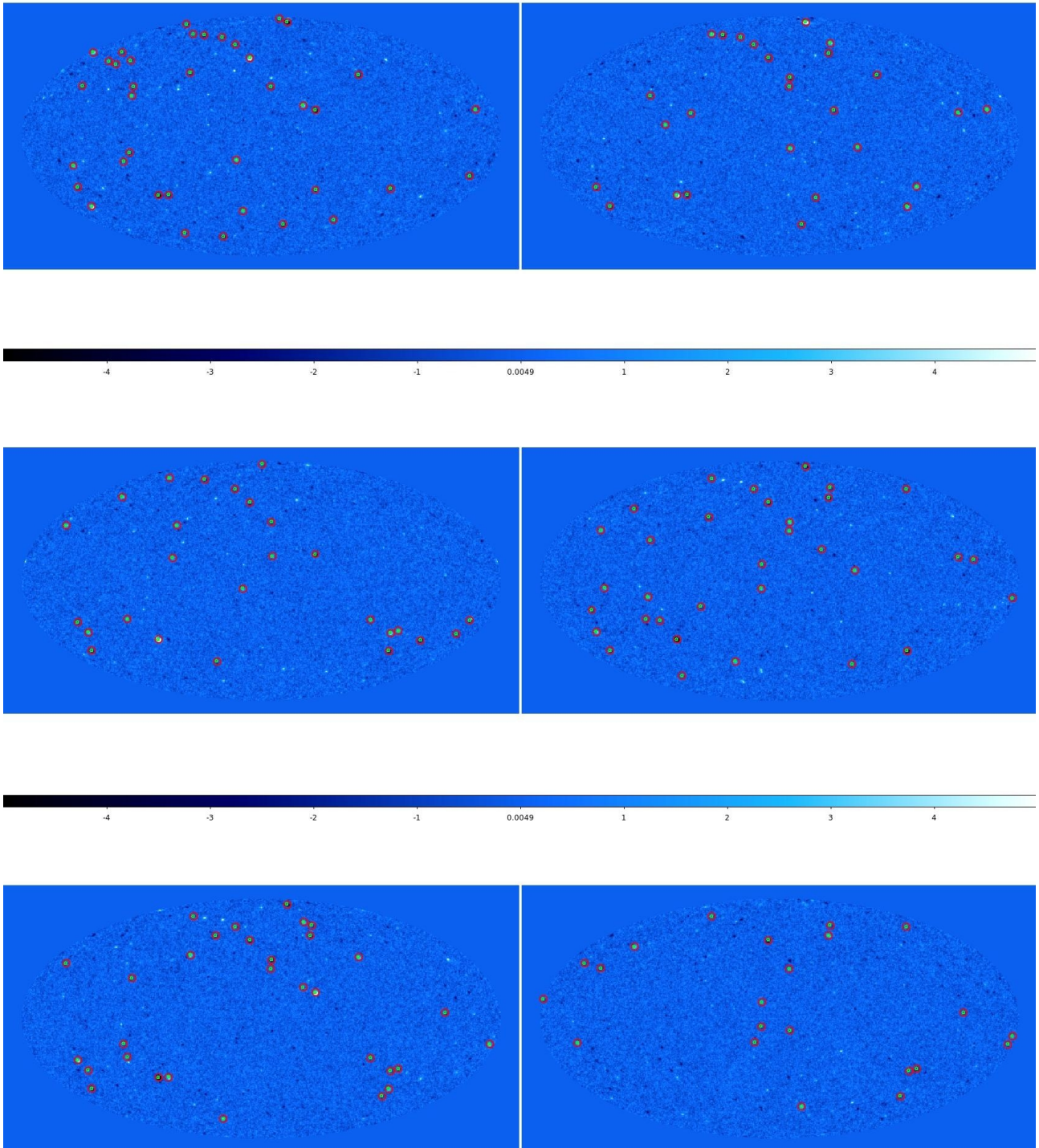
To identify the variable sources we applied the software SExtractor. This takes as input the counts difference map calculated by (1) and (2), the associated uncertainty map made by (3), and it gives as output the catalog of sources which have a variation of at least $\pm 5\sigma$ from the background which is weighted by our error map in eq. (3). The extracted sources must have a correspondent value of at least 5 in the significance map evaluated by (4).

Each annual catalog of variable sources has been compared with the 3FGL catalog. Then the seven catalogs have been collected in a unique catalog (VAR). All the sources of the VAR

have a correspondence on the 3FGL, except one, the number 82, extracted on year 7. A possible interpretation is given below.

Tool used: Fermi Science Tools (gtsrcid), sextractor, ds9, fv and python.

The following image shows year by year the VAR sources (red circles) and the 3FGL correspondent source (green circles).



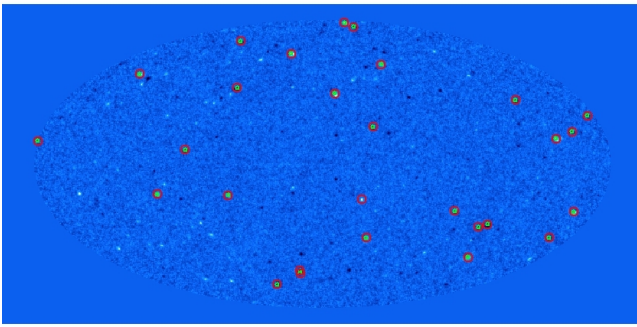


IMAGE 7. Annual significance maps with VAR sources (red circles) and associated 3FGL sources (green circles). From left to right map1-map2-map3, map4-map5-map6, map7.

Finally the VAR catalog for the all 7-year variable sources (green circles) is reported over a counts normalized with the exposure map of 7-year. The source not associated at the 3FGL catalog is in the red circle.

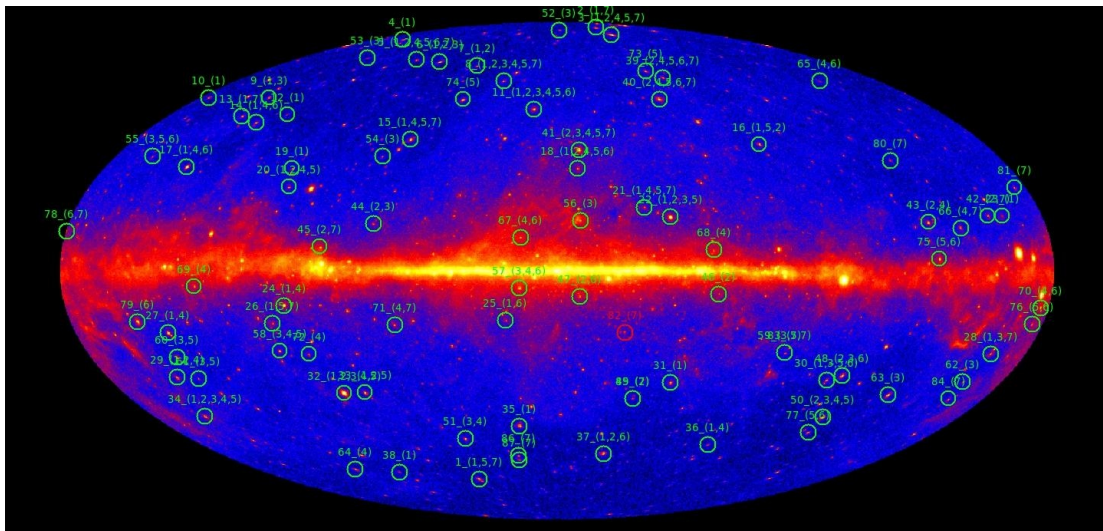


IMAGE 8. 7 year counts normalized with exposure map (energy range [1-500]GeV, $z_{max}=90deg$, event type=FRONT and BACK, event class=1024 (ultracleanveto), 0.3 deg bin size) and VAR catalog. In red the source not associated at the 3FGL catalog. In green the sources with a 3FGL counterpart. In brackets the years in which the source is extracted.

To have a quick check of the variation in time of the detected sources we report the light curve of some central sources. The time in the plots is expressed in MJD, the correspondence to the year separation adopted in this analysis is:

1: 2008/08/01 – 2009/08/01 = 54679 – 55044 (MJD)

2: 2009/08/01 – 2010/08/01 = 55044 – 55409 (MJD)

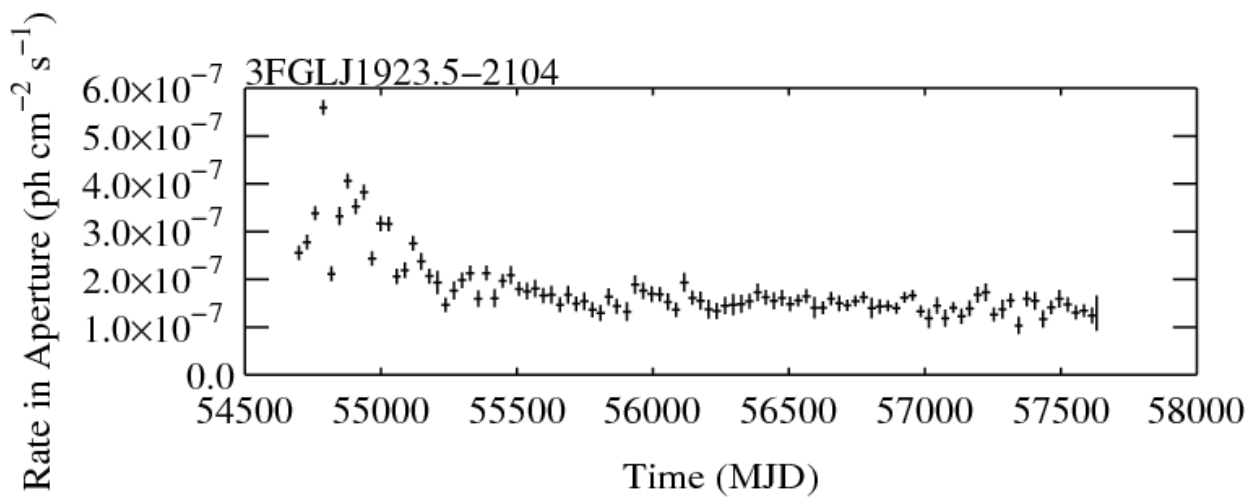
3: 2010/08/01 – 2011/08/01 = 55409 – 55774 (MJD)

4: 2011/08/01 – 2012/08/01 = 55774 – 56140 (MJD)

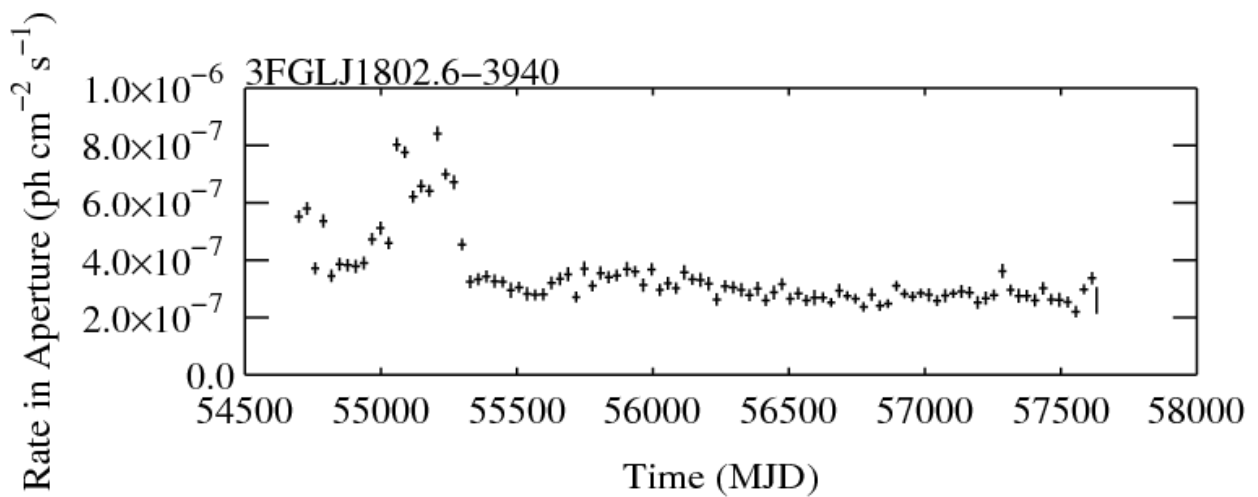
5: 2012/08/01 – 2013/08/01 = 56140 – 56505 (MJD)

6: 2013/08/01 – 2014/08/01 = 56505 – 56870 (MJD)

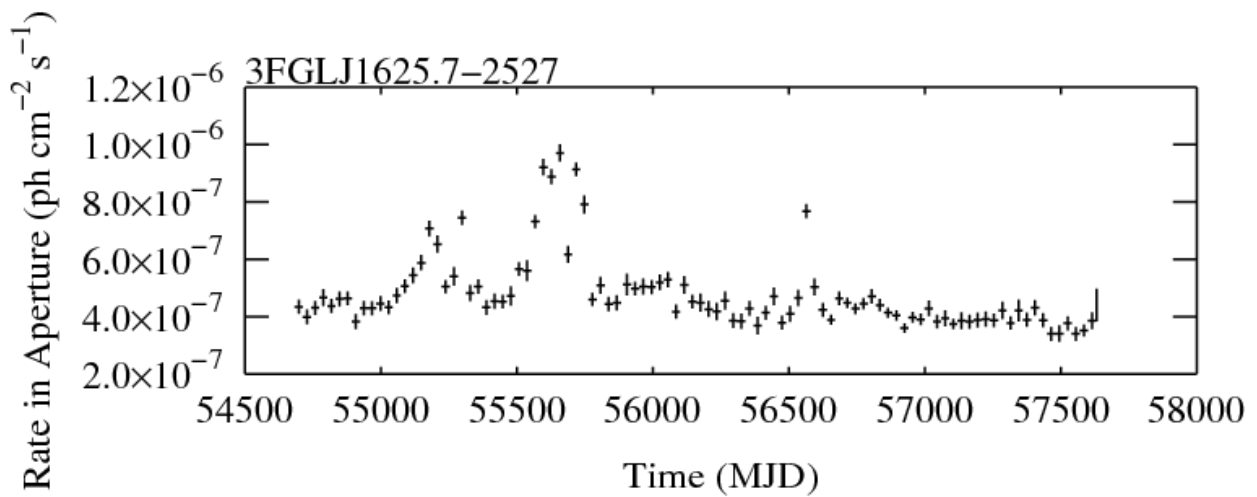
7: 2014/08/01 – 2015/08/01 = 56870 – 57235 (MJD)



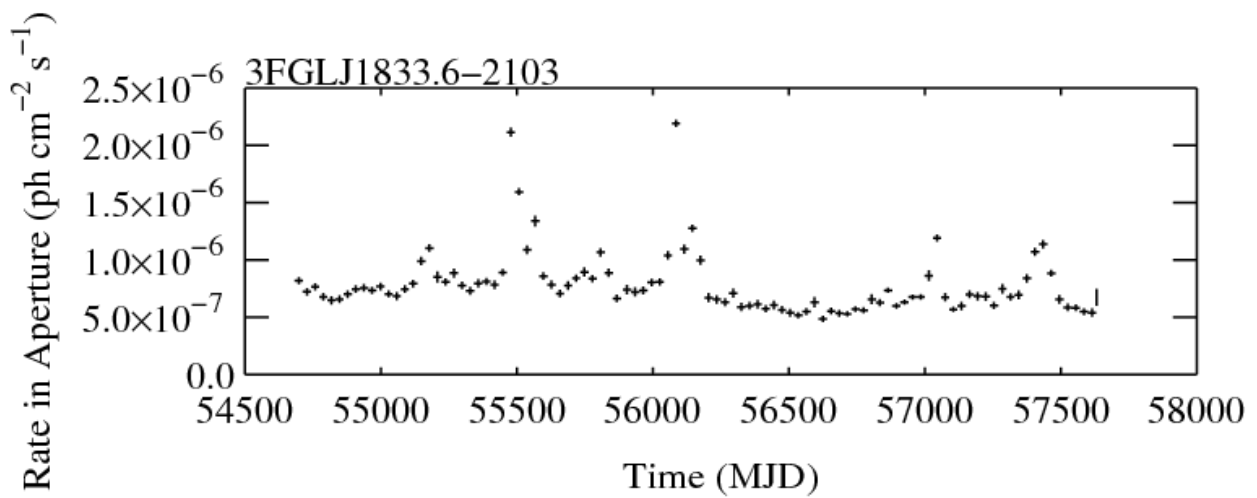
Source 25 of VAR



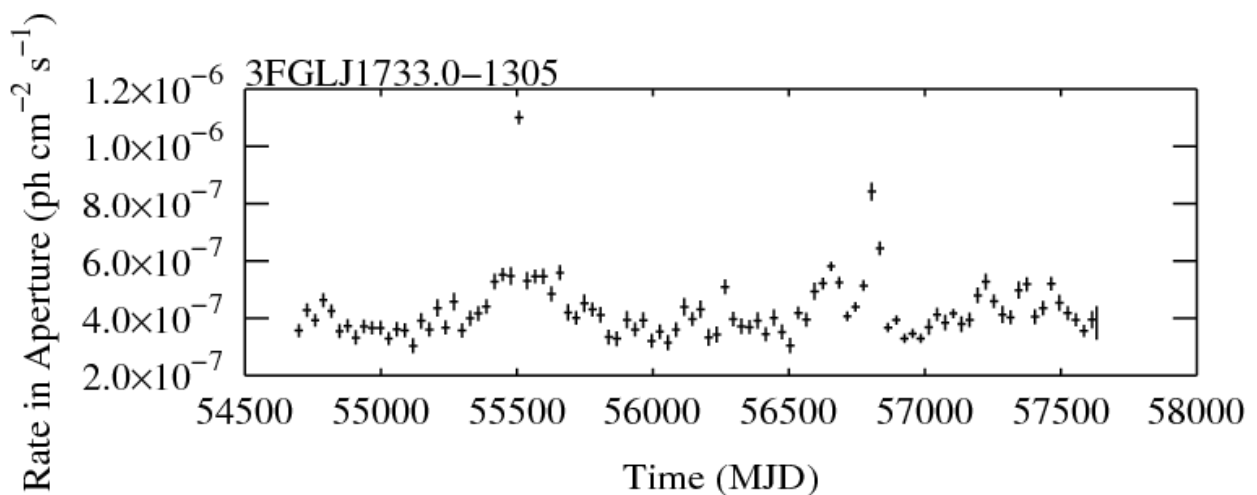
Source 47 of VAR



Source 56 of VAR



Source 57 of VAR



Source 67 of VAR

At the end of the report there is the full VAR catalog and the 3FGL association.

Source 82 of VAR

The applied Fermi Science Tool gtsrcid, which spatially associates the sources of VAR to a

counterpart in the 3FGL catalog, hasn't found any association for source 82. A histogram of the angular distance between VAR sources and the closest 3FGL source shows that the precision of the spatial association is contained in the resolution of the map (0.5 deg bin size). The angular distance between source 82 and the nearest 3FGL source is significantly larger than other sources allowing considering source 82 not associated.

Frequency
(all annual
catalogs)

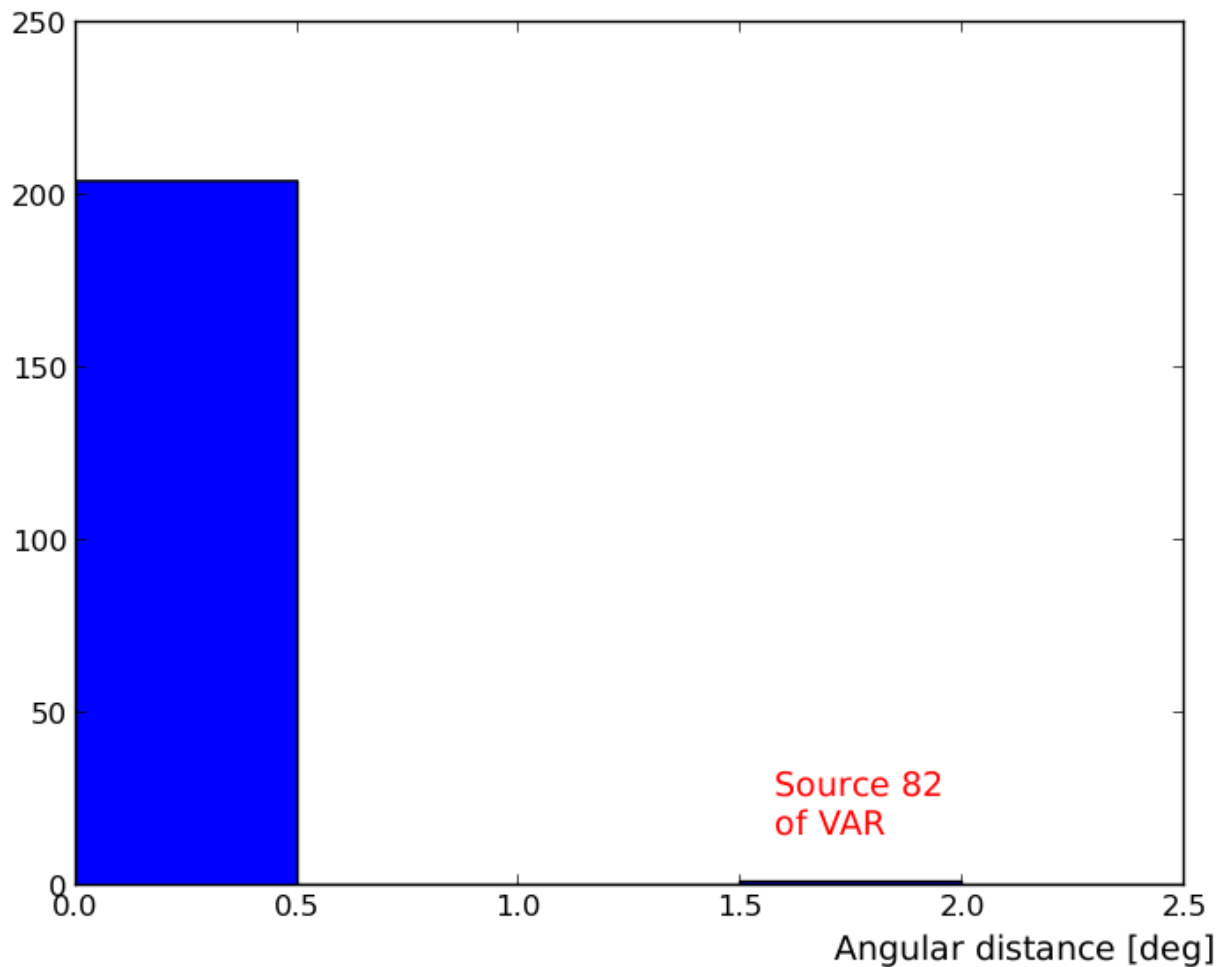


IMAGE 9. Histogram of the angular separation between VAR sources and the nearest 3FGL source.

Looking at the annual counts map normalized with the exposure it is possible to observe that source 82 of VAR emerges from the background between 2013 and 2015 (our 6th and 7th year). That may be the cause for which this source is not present in the 3FGL catalog, which has been done with only 4-year data. A check with the latest version of the Fermi-LAT catalog has to be done in future.

Conclusion and Observations

The catalog of annual variable sources was produced and compared with the 3FGL. All sources are associated with a source in the 3FGL. Source VAR 82 with a significant annual

variation does not have any 3FGL association. This will be studied in future works. We also found that the overall sky does not exhibit significant variation over the different years. In the Galactic center region (20degx20deg) 3 sources were found to have a significant 5-sigma variation.

VAR Catalog, 3FGL association, class of the source.

In brackets after the name of the VAR sources there is the year of extraction of the source.

- {VAR_NAME, 3FGL_NAME, class}{1_(1,5,7), 3FGL J2345.2-1554, FSRQ}
- {VAR_NAME, 3FGL_NAME, class}{2_(1,7), 3FGL J1230.3+2519, bll}
- {VAR_NAME, 3FGL_NAME, class}{3_(1,2,4,5,7), 3FGL J1224.9+2122, FSRQ}
- {VAR_NAME, 3FGL_NAME, class}{4_(1), 3FGL J1146.8+3958, fsrq}
- {VAR_NAME, 3FGL_NAME, class}{5_(1,2,4,5,6,7), 3FGL J1312.7+4828, agn}
- {VAR_NAME, 3FGL_NAME, class}{6_(1,2,3), 3FGL J1345.6+4453, fsrq}
- {VAR_NAME, 3FGL_NAME, class}{7_(1,2), 3FGL J1418.5+3543, BCU}
- {VAR_NAME, 3FGL_NAME, class}{8_(1,2,3,4,5,7), 3FGL J1443.9+2502, fsrq}
- {VAR_NAME, 3FGL_NAME, class}{9_(1,3), 3FGL J1033.8+6051, FSRQ}
- {VAR_NAME, 3FGL_NAME, class}{10_(1), 3FGL J0920.9+4442, fsrq}
- {VAR_NAME, 3FGL_NAME, class}{11_(1,2,3,4,5,6), 3FGL J1504.4+1029, FSRQ}
- {VAR_NAME, 3FGL_NAME, class}{12_(1), 3FGL J1220.2+7105, fsrq}
- {VAR_NAME, 3FGL_NAME, class}{13_(1,7), 3FGL J0958.6+6534, bll}
- {VAR_NAME, 3FGL_NAME, class}{14_(1,4,6), 3FGL J1048.4+7144, FSRQ}
- {VAR_NAME, 3FGL_NAME, class}{15_(1,4,5,7), 3FGL J1635.2+3809, FSRQ}
- {VAR_NAME, 3FGL_NAME, class}{16_(1,5,2), 3FGL J1127.0-1857, fsrq}
- {VAR_NAME, 3FGL_NAME, class}{17_(1,4,6), 3FGL J0721.9+7120, BLL}
- {VAR_NAME, 3FGL_NAME, class}{18_(1,2,4,5,6), 3FGL J1532.7-1319, bcu}
- {VAR_NAME, 3FGL_NAME, class}{19_(1), 3FGL J1748.6+7005, bll}
- {VAR_NAME, 3FGL_NAME, class}{20_(1,2,4,5), 3FGL J1849.2+6705, FSRQ}
- {VAR_NAME, 3FGL_NAME, class}{21_(1,4,5,7), 3FGL J1457.4-3539, FSRQ}
- {VAR_NAME, 3FGL_NAME, class}{22_(1,2,3,5), 3FGL J1427.9-4206, FSRQ}
- {VAR_NAME, 3FGL_NAME, class}{23_(1), 3FGL J0713.9+1933, fsrq}
- {VAR_NAME, 3FGL_NAME, class}{24_(1,4), 3FGL J2202.7+4217, BLL}

{VAR_NAME, 3FGL_NAME, class}{25_(1,6), 3FGL J1923.5-2104, fsrq}
{VAR_NAME, 3FGL_NAME, class}{26_(1,5,7), 3FGL J2244.1+4057, bll}
{VAR_NAME, 3FGL_NAME, class}{27_(1,4), 3FGL J0222.6+4301, BLL}
{VAR_NAME, 3FGL_NAME, class}{28_(1,3,7), 3FGL J0505.3+0459, fsrq}
{VAR_NAME, 3FGL_NAME, class}{29_(1,2,4), 3FGL J0237.9+2848, FSRQ}
{VAR_NAME, 3FGL_NAME, class}{30_(1,3,5,6), 3FGL J0532.0-4827, BCU}
{VAR_NAME, 3FGL_NAME, class}{31_(1), 3FGL J2147.3-7536, FSRQ}
{VAR_NAME, 3FGL_NAME, class}{32_(1,2,3,4,5), 3FGL J2254.0+1608, FSRQ}
{VAR_NAME, 3FGL_NAME, class}{33_(1,2,5), 3FGL J2232.5+1143, FSRQ}
{VAR_NAME, 3FGL_NAME, class}{34_(1,2,3,4,5), 3FGL J0238.6+1636, BLL}
{VAR_NAME, 3FGL_NAME, class}{35_(1), 3FGL J2158.8-3013, bll}
{VAR_NAME, 3FGL_NAME, class}{36_(1,4), 3FGL J0228.3-5545, fsrq}
{VAR_NAME, 3FGL_NAME, class}{37_(1,2,6), 3FGL J2329.3-4955, fsrq}
{VAR_NAME, 3FGL_NAME, class}{38_(1), 3FGL J0030.7-0209, bcu}
{VAR_NAME, 3FGL_NAME, class}{39_(2,4,5,6,7), 3FGL J1229.1+0202, FSRQ}
{VAR_NAME, 3FGL_NAME, class}{40_(2,4,5,6,7), 3FGL J1256.1-0547, FSRQ}
{VAR_NAME, 3FGL_NAME, class}{41_(2,3,4,5,7), 3FGL J1512.8-0906, FSRQ}
{VAR_NAME, 3FGL_NAME, class}{42_(2,7), 3FGL J0725.2+1425, FSRQ}
{VAR_NAME, 3FGL_NAME, class}{43_(2,4), 3FGL J0808.2-0751, fsrq}
{VAR_NAME, 3FGL_NAME, class}{44_(2,3), 3FGL J1848.4+3216, FSRQ}
{VAR_NAME, 3FGL_NAME, class}{45_(2,7), 3FGL J2001.1+4352, bll}
{VAR_NAME, 3FGL_NAME, class}{46_(2), 3FGL J1330.1-7002, bcu}
{VAR_NAME, 3FGL_NAME, class}{47_(2,6), 3FGL J1802.6-3940, fsrq}
{VAR_NAME, 3FGL_NAME, class}{48_(2,3,6), 3FGL J0538.8-4405, BLL}
{VAR_NAME, 3FGL_NAME, class}{49_(2), 3FGL J2141.6-6412, bcu}
{VAR_NAME, 3FGL_NAME, class}{50_(2,3,4,5), 3FGL J0428.6-3756, bll}
{VAR_NAME, 3FGL_NAME, class}{51_(3,4), 3FGL J2236.5-1432, BLL}
{VAR_NAME, 3FGL_NAME, class}{52_(3), 3FGL J1303.0+2435, bll}
{VAR_NAME, 3FGL_NAME, class}{53_(3), 3FGL J1153.4+4932, FSRQ}

{VAR_NAME, 3FGL_NAME, class}{54_(3), 3FGL J1709.6+4318, fsrq}
{VAR_NAME, 3FGL_NAME, class}{55_(3,5,6), 3FGL J0742.6+5444, fsrq}
{VAR_NAME, 3FGL_NAME, class}{56_(3), 3FGL J1625.7-2527, fsrq}
{VAR_NAME, 3FGL_NAME, class}{57_(3,4,6), 3FGL J1833.6-2103, fsrq}
{VAR_NAME, 3FGL_NAME, class}{58_(3,4,5), 3FGL J2311.0+3425, FSRQ}
{VAR_NAME, 3FGL_NAME, class}{59_(3,5,7), 3FGL J0644.3-6713, bcu}
{VAR_NAME, 3FGL_NAME, class}{60_(3,5), 3FGL J0221.1+3556, FSRQ}
{VAR_NAME, 3FGL_NAME, class}{61_(3,5), 3FGL J0203.6+3043, bll}
{VAR_NAME, 3FGL_NAME, class}{62_(3), 3FGL J0442.6-0017, fsrq}
{VAR_NAME, 3FGL_NAME, class}{63_(3), 3FGL J0457.0-2324, FSRQ}
{VAR_NAME, 3FGL_NAME, class}{64_(4), 3FGL J0108.7+0134, fsrq}
{VAR_NAME, 3FGL_NAME, class}{65_(4,6), 3FGL J1012.6+2439, fsrq}
{VAR_NAME, 3FGL_NAME, class}{66_(4,7), 3FGL J0739.4+0137, fsrq}
{VAR_NAME, 3FGL_NAME, class}{67_(4,6), 3FGL J1733.0-1305, FSRQ}
{VAR_NAME, 3FGL_NAME, class}{68_(4), 3FGL J1328.9-5607, bcu}
{VAR_NAME, 3FGL_NAME, class}{69_(4), 3FGL J0102.8+5825, fsrq}
{VAR_NAME, 3FGL_NAME, class}{70_(4,6), 3FGL J0521.7+2113, bll}
{VAR_NAME, 3FGL_NAME, class}{71_(4,7), 3FGL J2035.3+1055, fsrq}
{VAR_NAME, 3FGL_NAME, class}{72_(4), 3FGL J2236.3+2829, bll}
{VAR_NAME, 3FGL_NAME, class}{73_(5), 3FGL J1239.5+0443, fsrq}
{VAR_NAME, 3FGL_NAME, class}{74_(5), 3FGL J1522.1+3144, fsrq}
{VAR_NAME, 3FGL_NAME, class}{75_(5,6), 3FGL J0730.2-1141, fsrq}
{VAR_NAME, 3FGL_NAME, class}{76_(5,6), 3FGL J0510.0+1802, fsrq}
{VAR_NAME, 3FGL_NAME, class}{77_(5,6), 3FGL J0403.9-3604, FSRQ}
{VAR_NAME, 3FGL_NAME, class}{78_(6,7), 3FGL J0622.9+3326, BCU}
{VAR_NAME, 3FGL_NAME, class}{79_(6), 3FGL J0319.8+4130, RDG}
{VAR_NAME, 3FGL_NAME, class}{80_(7), 3FGL J0909.1+0121, fsrq}
{VAR_NAME, 3FGL_NAME, class}{81_(7), 3FGL J0719.3+3307, fsrq}
{VAR_NAME, 3FGL_NAME, class}{82_(7)}

{VAR_NAME, 3FGL_NAME, class}{83_(7), 3FGL J0644.3-6713, bcu}

{VAR_NAME, 3FGL_NAME, class}{84_(7), 3FGL J0423.2-0119, FSRQ}

{VAR_NAME, 3FGL_NAME, class}{85_(7), 3FGL J2141.6-6412, bcu}

{VAR_NAME, 3FGL_NAME, class}{86_(7), 3FGL J2250.7-2806, bcu}

{VAR_NAME, 3FGL_NAME, class}{87_(7), 3FGL J2258.0-2759, fsrq}